Polymer 50 (2009) 6312–6322

Contents lists available at ScienceDirect

Polymer

journal homepage: www.elsevier.com/locate/polymer

Amorphous phase and crystalline morphology in blend of two polymorphic polyesters: Poly(hexamethylene terephthalate) and poly(heptamethylene terephthalate)

Kai Cheng Yen [a], Eamor M. Woo [a,*], Kohji Tashiro [b,**]

[a] Department of Chemical Engineering, National Cheng Kung University, Tainan, 701, Taiwan
[b] Department of Future Industry-oriented Basic Science and Materials, Toyota Technological Institute, Tempaku, Nagoya 468-8511, Japan

ARTICLE INFO

Article history:
Received 27 July 2009
Received in revised form
20 October 2009
Accepted 29 October 2009
Available online 3 November 2009

Keywords:
Morphology
Miscibility
Polymorphism

ABSTRACT

Crystalline/crystalline blends of two polymorphic aryl-polyesters, poly(hexamethylene terephthalate) (PHT) and poly(heptamethylene terephthalate) (PHepT), were prepared and the crystallization kinetics, polymorphism behavior, spherulite morphology, and miscibility in this blend system were probed using polarized-light optical microscopy (POM), differential scanning calorimetry (DSC), temperature-resolved wide-angle X-ray diffraction (WAXD), and small angle X-ray scattering (SAXS). The PHT/PHepT blends of all compositions were proven to be miscible in the melt state or quenched amorphous glassy phase. Miscibility in PHT/PHepT blend leads to the retardation in the crystallization rate of PHT; however, that of PHepT increases, being attributed to the nucleation effects of PHT crystals which are produced before the growth of PHepT crystals. In the miscible blend of polymorphic PHT with polymorphic PHepT, the polymorphism states of both PHT and PHepT in the blend are influenced by the other component. The fraction of the thermodynamically stable β-crystal of PHT in the blend increases with increasing PHepT content when melt-crystallized at 100 °C. In addition, when blended with PHT, the crystal stability of PHepT is altered and leads to that the originally polymorphic PHepT exhibits only the β-crystal when melt-crystallized at all T_c's. Apart from the noted polymorphism behavior, miscibility in the blend also shows great influence on the spherulite morphology of PHT crystallized at 100 °C, in which the dendritic morphology corresponding to the β-crystal of PHT changes to the ring-banded in the blend with higher than 50 wt% PHepT. In blends of PHT/PHepT one-step crystallized at 60 °C, PHepT is located in both PHT interlamellar and interfibrillar region analyzed using SAXS, which further manifests the miscibility between PHT and PHepT.

1. Introduction

Miscibility and crystallization behavior in blends comprising aryl-polyesters have been widely studied, such as poly(ethylene terephthalate) (PET)/poly(trimethylene terephthalate) (PTT) [1], poly(butylene terephthalate) (PBT)/PTT [1], PBT/PET [2], poly(hexamethylene terephthalate) (PHT)/poly(pentamethylene terephthalate) (PPT) [3] and PPT/poly(heptamethylene terephthalate) (PHepT) [4]. All blend systems mentioned above are miscible in the glassy and melt states [1–4]. In addition to the binary blends mentioned above, a ternary blend of PET/PTT/PBT has also been proven to be miscible [5]. Note that, these aryl-polyesters are of the same functional groups but differ in the number of the methylene group in the repeating units of main chain. Most commercially interested aryl-polyesters, such as PET, PBT, PTT, and PPT are monomorphic polymers exhibiting only one crystal form in melt crystallization. In contrast, PHT and PHepT are polymorphic polymers exhibiting two or three crystal forms under different crystallization conditions. PHT shows mixed and variable fractions of α- and β-crystals in melt crystallization at T_c lower than 140 °C and sole β-crystal at T_c higher than 140 °C [6,7]. The polymorphic behavior in PHepT depends on T_{max} (the maximum melting temperature) and crystallization temperature (T_c) [8,9]. Aryl-polyesters varying in the repeat units can assume different crystal cells and some are monomorphic (single crystal cell) while others are polymorphic (more than one cell type). The earlier studies on the miscible PTT/PET, PTT/PBT, and PET/PTT/PBT blends were monomorphic/monomorphic cases, whereas the PPT/PHT and PPT/PHepT blends were monomorphic/polymorphic cases. By contrast, the present study on the PHT/PHepT blend was a more complex polymorphic/polymorphic system.

* Corresponding author.
** Corresponding author.
E-mail addresses: emwoo@mail.ncku.edu.tw (E.M. Woo), ktashiro@toyota-ti.ac.jp (K. Tashiro).

0032-3861/$ – see front matter © 2009 Elsevier Ltd. All rights reserved.
doi:10.1016/j.polymer.2009.10.066

Semicrystalline/semicrystalline blends, especially those with polymorphic crystal cells, can exhibit a quite complex phase behavior. At temperatures between the melting points of two components, the blend is actually a semicrystalline/amorphous system, and the amorphous component can be incorporated in the interlamellar, interfibrillar or rejected from the spherulites (interspherulitic). Interlamellar inclusion or incorporation means that in a miscible semicrystalline/amorphous blend, the amorphous component is located between the alternatively arranged lamellar crystals of the semicrystalline one. Interfibrillar segregation indicates that the amorphous component is located between the lamellar stacks of the semicrystalline polymer. In addition, interspherulite segregation means that the amorphous component is rejected from the spherulites of the semicrystalline polymers and resides between the spherulites. Penning et al. [10,11] have reported that in the miscible poly(butylene adipate) (PBA)/poly(vinylidene fluoride) (PVF_2) blend, at temperature between the melting temperatures of PBA and PVF_2 ($T_{m,PBA} < T < T_{m,PVF2}$) leading to a semicrystalline/amorphous state, the PBA component is mainly incorporated in the interlamellar region for the blends containing less than 50 wt% PBA. However, if the PBA content is higher than 50 wt%, interlamellar inclusion changes to interspherulitic segregation judged from the nonlinear spherulite growth rates of PVF_2 in the blends [12]. In miscible poly(ethylene oxide) (PEO)/poly(ethylene succinate) (PESu), both crystallization processes via direct cooling to 70 °C (where only PESu is crystallized) and direct cooling to 40 °C (where two components are crystallized simultaneously) followed by heating to 68 °C (to melt PEO crystals) create a high extent of interfibillar segregation coupled with a minor extent of interlamellar incorporation of amorphous PEO [13]. In the semicrystalline/amorphous state of PC/PCL blend (above T_m of PCL), PCL is incorporated in the PC interlamellar region in the PC-rich blends; however, in the PCL-rich blend, PCL is rejected from the PC interlamellar region [14]. The transition from interlamellar inclusion to interlamellar exclusion in the PC/PCL blend is postulated to be related to the changes in the T_g value of the blends leading to the changes in the chain diffusivity [14].

Phase behavior and crystalline morphology of blends comprising two polymorphic semicrystalline aryl-polyesters with long methylene segments [–$(CH_2)_n$– with $n = 6$ or 7] in repeating units have been less studied. Polymorphism including three crystal forms in PHT had been earlier disclosed more thoroughly [15–17], but crystal analyses on polymorphism related to PHePT were only recently studied and disclosed in a few publications [8,9,18]. In this study, PHT/PHepT blends were investigated with two objectives. First, both are crystalline and polymorphous but with different T_m's; thus, effect of another species on spherulitic morphology, crystallization kinetics and polymorphism could be assessed. Secondly, PHT/PHepT blend samples, one-step crystallized at 60 °C, were prepared for SAXS analysis at 25 °C and 100 °C to reveal the spatial distribution of lamellae in PHepT. In the PHT/PHepT blend, T_g of the blend changes with composition only slightly because the glass transition temperatures of PHT (−6.7 °C) and PHepT (−1.6 °C) are very close. The almost invariability of the PHT/PHepT blend on composition means that the chain mobility of the blend is not changed significantly. Thus, this system served as a good model to further study on the spatial distribution of the low-T_m component (PHepT) in the crystalline/crystalline blends with closely-spaced T_g.

2. Experimental

2.1. Materials

Poly(hexamethylene terephthalate) (PHT) and Poly(heptamethylene terephthalate) (PHepT) were not commercially available and were synthesized in-house using a catalyst (butyl titanate) by the method described earlier in the literature [19]. Characterizations showed basic physical data for PHepT, whose $T_g = -1.6$ °C, $T_m = 96$ °C, $M_w = 37{,}500$ g/mol (GPC), and polydispersity index (PDI) = 1.7 (GPC). The basic physical data for PHT are $T_g = -6.7$ °C, $T_m = 144$ °C, $M_w = 13{,}800$ g/mol, and PDI = 2.0.

PHT and PHepT were first weighed with intended weight ratios, respectively, and co-dissolved into chloroform solvent (2 wt%) with continuous stirring with a magnetic bar. Subsequently, the polymer solution was poured into a flat aluminum mold or glass Petri dishes at ambient temperature (25 °C). After evaporation of solvent at ambient temperature, all blend samples were later subjected to a vacuum oven at 60 °C for 7 days to ensure complete removal of residual solvent. The temperature used to remove the residual solvent (60 °C) in vacuum was not high and thus possible high temperature-induced reactions (*trans*-esterifications, etc) or possible degradation of these two polyesters was not likely to occur.

2.2. Apparatus

2.2.1. Differential scanning calorimetry (DSC)

DSC measurements were made in a Perkin–Elmer DSC-Diamond equipped with a mechanical intracooler under nitrogen purge. Temperature and heat flow calibrations at different heating rates were done using indium and zinc. Scanning rates of 20 °C/min, 10 °C/min, and −10 °C/min were used whenever needed. For T_g characterization, all DSC runs were performed on samples that were heated to melt and then rapidly quenched to liquid nitrogen to attain amorphous states (with crystallinity suppressed as much as possible) prior to the DSC scanning.

2.2.2. Polarized optical microscopy (POM)

A Nikon Optiphot-2 polarized-light optical microscope (POM) equipped with a charge-coupled device (CCD) digital camera and a Linkam THMS-6000 microscopic heating stage with TP-92 temperature programmer was used to observe the crystal morphology and the phase behavior of the blend samples. Thin films of the specimens for the investigations on the phase behavior of the blends were sandwiched between two glass slides. However, thin-film specimens for the investigations on the crystalline morphology were cast onto one glass slide without cover. The melt-crystallized blend samples were melted at 180 °C for 5 min and then rapidly cooled to the intended crystallization temperature (T_c) by replacing the molten sample (on micro glass slide) onto a hot stage with a preset isothermal temperature.

2.2.3. Temperature-resolved wide-angle X-ray diffraction (WAXD)

A Rigaku X-ray diffraction RINT-TTR III was used for the in-situ WAXD measurement of the heating process in the blend samples from the crystallization temperature (100 °C). The X-ray beam used was CuK_α radiation. The X-ray powder patterns were measured in the 2θ ranges of 15°–25°, and the heating rate was 1 °C/min.

2.2.4. Small-angle X-ray scattering (SAXS)

A Rigaku Nanoviewer high brilliant small angle X-ray scattering system was used for SAXS measurement for blend samples at ambient temperature (25 °C) and heated at 100 °C and a Rigaku Dectris detector (Pilatus) was used to record the scattering signals. The X-ray beam used was CuK_α radiation ($\lambda = 0.1542$ nm). X-ray powder patterns were measured in the small 2θ range of 0.15°–1.2°. The scattering intensity $I(q)$ was transformed to $I(q)q^2$ for the correction of Lorentz factor, where q is a scattering vector defined

as $q = (4\pi/\lambda)\sin\theta$ (λ is wavelength of incident X-ray beam and 2θ is scattering angle).

3. Results and discussion

3.1. Miscibility in PHT/PHepT blend

First, miscibility in the crystalline/crystalline PHT/PHepT blend was proven by observing relevant evidence. The crystalline domains of the blends were examined using POM. Fig. 1 shows POM/OM micrographs of PHT/PHepT blends in five different compositions (90/10, 70/30, 50/50, 30/70 and 10/90) (A) as cast at ambient temperature (25 °C) and (B) heated to melt (180 °C) with heating rate = 2 °C/min. In each composition, POM micrograph shows small crystals in the as-cast sample, and upon heating to melt, OM micrograph shows a transparent and homogeneous phase. Note that, at this temperature (180 °C), trans-reactions or trans-esterifications between the polyesters were not likely, and the blend remained as a physically well mixed liquid mixture system, without any chemical reactions. These blends were later

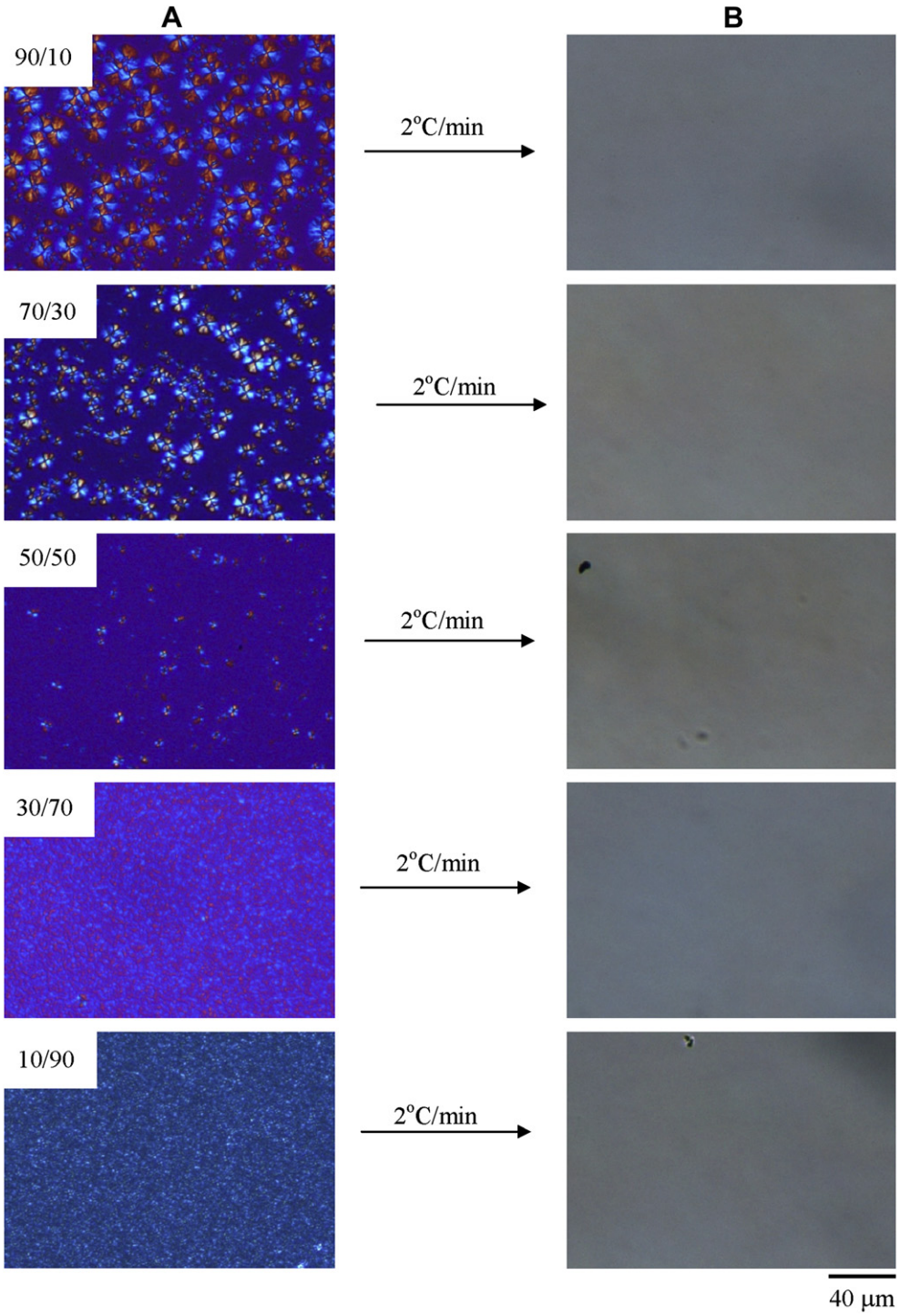

Fig. 1. POM/OM micrographs for PHT/PHepT blends (five compositions in each of Columns A, B): (A) as-cast and (B) melt at 180 °C.

heated to as high as 300 °C and the homogeneous phases remained unchanged at higher temperatures until thermal degradation (not shown for brevity).

DSC characterization was then performed to get further evidence of the phase behavior of PHT/PHepT blends of different compositions using the blend T_g criteria. Fig. 2 shows DSC thermograms of PHT/PHepT blends scanned from −20 °C (amorphous state) to 180 °C (molten state) with scanning rate = 20 °C/min. The glass transition temperatures of PHT ($T_g = -6.7$ °C) and PHepT ($T_g = -1.6$ °C) are considerably close and it is thus difficult to determine the miscibility of this blend system based on the criterion of single glass transition temperature. However, other thermal characteristics can support the evidence in determination of the miscibility in this blend. The cold-crystallization peak ($T_{c.c.}$) of neat PHT is at 10 °C and shifts to higher temperature when blended with PHepT, which indicates that the crystallization rate of PHT is depressed due to the intimate mixing between PHT and PHepT. In contrast to the suppression of the crystallization rate in PHT when blended with PHepT, that of PHepT is enhanced upon blending with PHT even with a small fraction of PHT (10 wt%). The DSC trace of neat PHepT shows only an apparent glass transition temperature, while the cold-crystallization peak as well as the melting peak are absent due to the slow crystallization rate of PHepT. However, when blended with a small fraction of PHT (PHT/PHepT = 10/90 and 30/70), the cold-crystallization peak corresponding to PHepT appears. In PHT/PHepT = 30/70, the DSC trace shows two partially merged exothermic peaks attributed to the crystallization of PHT and PHepT during scanning. Although precise correspondence of these two exothermic peaks to lamellae in PHT or PHepT is not yet known, it is true that the crystallization rate of PHepT is enhanced by judging from the increased endothermic enthalpy of the melting peak of PHepT during the same scanning process. In PHT/PHepT = 10/90 blend, the cold-crystallization peak at 50 °C is attributed to both PHT and PHepT which is clarified by the nearly equal value of the exothermic enthalpy ($\Delta H_c = 29.6$ J/g) and the total endothermic enthalpy of PHT ($\Delta H_{f,\ PHT} = 3.8$ J/g) and PHepT ($\Delta H_{f,\ PHT} = 26.3$ J/g). Besides, the DSC curves of PHT/PHepT = 10/90 and 30/70, where the cold-crystallization occurs at around 50 °C and lower than 40 °C, respectively, show different melting endothermic profile. In PHT/PHepT = 10/90, the DSC curve shows the double melting peaks, while in PHT/PHepT = 30/70, only single melting peak is observed which is because that the melting behavior of PHepT is temperature-dependent. When $T_{c.c}$ is higher or lower than 40 °C, PHepT shows the double and single melting endothermic peaks, respectively, which is clarified by comparing with the DSC endotherm of non-isothermal cold crystallized PHepT at various temperature of which the heating rate from the quenched amorphous state is 20 °C/min which is same with that used in DSC scanning shown earlier in Fig. 2. Data are not duplicately shown here for similarity. Consequently, the increase in the intensity of the cold-crystallization peak of PHepT in the blend during scanning indicates that when blended with PHT, the crystallization rate of PHepT is enhanced. The melting temperature of PHT in each blend composition decreases with the increase of PHepT content because the crystal/lamellar packing of PHT is disrupted upon blending with PHepT leading to a lower thermal stability and melting temperature of PHT.

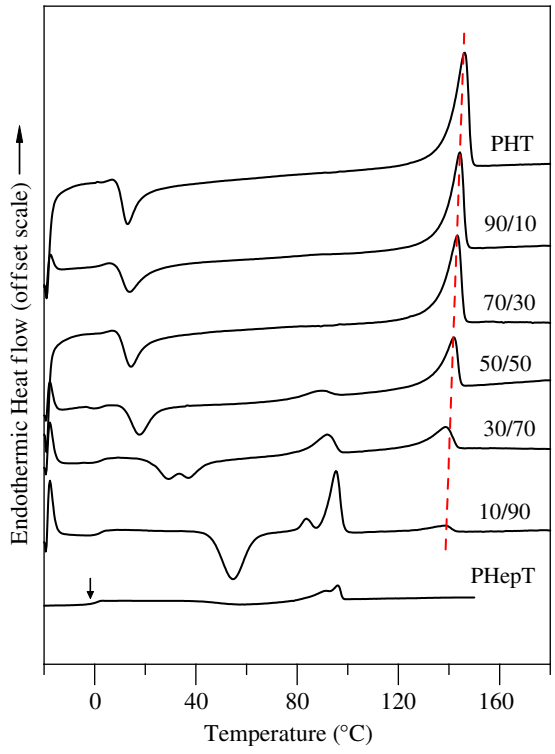

Fig. 2. DSC traces for quenched PHT/PHepT blends of different compositions (scanning rate = 20 °C/min).

3.2. Crystallization and polymorphic behavior in PHT/PHepT blend

In order to fully understand the mutual effect of PHT or PHepT content on the crystallization rate of the other component (PHepT or PHT), DSC was applied to analyze the non-isothermal crystallization process in PHT/PHepT blend cooled from melt ($T_{max} = 180$ °C) to −20 °C at cooling rate = −10 °C/min. Fig. 3 shows DSC thermograms of non-isothermal crystallization in PHT/PHepT blends by cooling from 180 °C to −20 °C ($R = -10$ °C/min). The crystallization exothermic peak during cooling in neat PHT is at 120 °C and shifts to lower temperatures when blended with PHepT. It further manifests that the crystallization rate of PHT is reduced due to the intimate mixing between PHT and PHepT. In all blend compositions, the crystallization of PHT during cooling from melt occurs at temperature higher than the melting temperature of PHepT (96 °C), which suggests that when PHT is crystallized, PHepT remains in the melt state and is well mixed with the amorphous PHT due to the miscibility between PHT and PHepT. Thus, the intimate chain mixing between PHT and PHepT leads to the retarded crystallization rate of PHT. In the DSC trace of neat PHepT, there is no exothermic peak observed upon scanning from melt to −20 °C, suggesting that nearly no crystal produced during this cooling process. However, in PHT/PHepT blends except for PHT/PHepT = 90/10, apart from the exothermic peak of PHT at higher temperature, another peak at nearly 60 °C is observed in each composition. In order to investigate the correlation between the lower exothermic peak at 60 °C and the component in the blend, the PHT/PHepT blend samples after being cooled from 180 °C to 50 °C were subsequently scanned with 10 °C/min to 180 °C. In all blend compositions, the heating traces show two melting peaks corresponding to PHT and PHepT, indicating that the crystallization peak at 60 °C is attributed to crystalline PHepT species (not shown for brevity). Thus, when blended with PHT, the crystallization rate of PHepT is increased. The T_g value of neat PHepT and the blends are almost of no variance and it is suggested that change of the chain mobility of PHepT in the blend with PHT is negligible and not the dominant factor leading to the increase of the crystallization rate of PHepT. In addition, PHepT in the blend is crystallized in the presence of PHT crystals. Thus, the increase of the crystallization rate of PHepT when blended with PHT may be due to the nucleation effect of PHT crystals produced before the crystallization of PHepT.

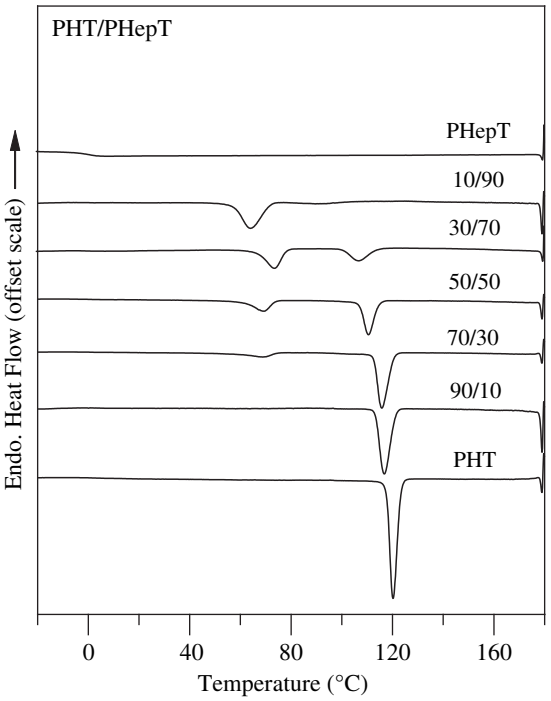

Fig. 3. Non-isothermal crystallization process in PHT/PHepT blends cooled from 180 °C to −20 °C at 10 °C/min.

PHT and PHepT are both polymorphous and exhibit multiple melting behavior in samples melt-crystallized. PHT shows the mixed α- and β-crystal and sole β-crystal in melt crystallization at T_c lower and higher than 140 °C, respectively. In addition, PHT shows as many as five melting peaks, P_1, P_2, P_3, P_4 and P_5 in melt crystallization at lower T_c (90 and 100 °C) scanned with 10 °C/min. The multiple melting behavior in melt-crystallized PHT is due to the polymorphism (mixture of the α- and β-crystal) and melting/recrystallization/remelting mechanism [6]. Among the melting peaks, P_1 and P_3 are attributed to the α-crystal, whereas P_2 and P_5 are attributed to the β-crystal. Besides, P_4 is the melting peak of the perfect and thickest lamellae packed by the α-crystal and the P_4 crystal transforms to the β-crystal through melting/recrystallization process and then merges with P_5 upon further annealing [6]. The influence of the amorphous PHepT chains on the polymorphism and multiple melting behavior of PHT were then characterized using DSC and WAXD.

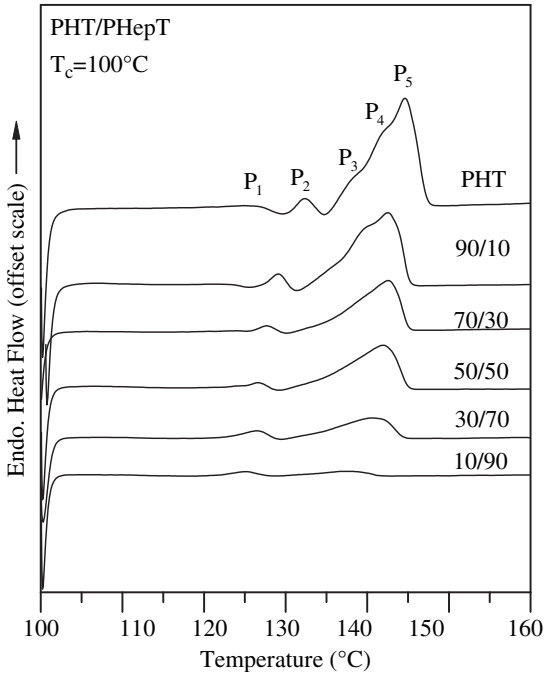

Fig. 4. DSC thermograms of PHT/PHepT blends melt-crystallized at 100 °C scanned 10 °C/min.

Fig. 4 shows DSC thermograms of PHT/PHepT blends melt-crystallized at $T_c = 100$ °C (above the melting temperature of PHepT) scanned with $R = 10$ °C/min. At this temperature (100 °C), PHT is crystallizable whereas PHepT is in the molten state and well mixed with the amorphous PHT chains leading to a two-phase system (the PHT crystalline phase and homogeneous amorphous phase). In Fig. 4, neat PHT crystallized at $T_c = 100$ °C shows five melting peaks (P_1, P_2, P_3, P_4 and P_5) as scanned with $R = 10$ °C/min. In PHT/PHepT = 90/10, these five melting peaks are distinctly observed, but the temperatures of all melting peaks shift to lower temperatures. However, when the PHepT content is higher than 30 wt%, P_1 and P_3 corresponding to the α-crystal become indistinguishable and only P_2 and P_5 corresponding to the β-crystal are apparently observed. It is supposed that the crystallization of the α-crystal of PHT is suppressed when blended with PHepT. Subsequently, WAXD characterization was performed to clarify the effect of the miscibility in the blends on the polymorphism in melt-crystallized PHT.

Fig. 5 shows WAXD diffractograms of PHT/PHepT blends melt-crystallized at $T_c = 100$ °C (1 h) measured at 100 °C, at which only PHT is crystallizable. The WAXD diffractogram of neat PHT at 100 °C shows both diffraction peaks corresponding to the α-($2\theta = 15.9°$, 20.5°, 21.2° and 25.4°) and β-crystal ($2\theta = 15.8°$, 17.9° and 23.6°). Besides, the α-crystal is of a higher fraction than β-crystal judged from the relative intensity of the diffraction peak of the α- and β-crystal. However, when blended with PHepT, the relative intensity of the diffraction peaks at $2\theta = 17.9°$ (β-crystal) to that at $2\theta = 21.2°$ (α-crystal) increases with increasing PHepT content, which indicates that the crystallization of the α-crystal of PHT is depressed in the miscible PHT/PHepT blend. Among the different modifications of a given polymorphic polymer, there is usually a polymorph which is thermodynamically the most stable, corresponding to the crystal formed under the usual crystallization conditions. The β-crystal of melt-crystallized PHT is of the higher melting temperature in comparison to that of the α-crystal and crystallized at higher crystallization temperatures. Thus, the β-crystal is of the higher thermodynamic stability and α-crystal is more kinetically favorable. When blended with PHepT, the fraction of the more stable β-crystal of PHT increases, due to the blending effects of PHepT on the thermodynamic and kinetics environment of PHT crystallization.

PHepT is also a polymorphic polymer exhibiting the α- and β-crystal depending on T_{max} and T_c [8,9]. A lower $T_{max} = 110$ °C leads to a heterogeneous nucleation and crystallization of the α-crystal due to insufficient melting of the residual α-nuclei at this low T_{max}. By contrast, when heated at a T_{max} higher than 150 °C (in this study, $T_{max} = 180$ °C was used), all the residual nuclei are erased and the polymorphic behavior is dependent on T_c, in which PHepT is packed into the α-crystal at T_c lower than 25 °C and β-crystal at T_c higher than 35 °C, respectively. From the results shown in Fig. 3, it is known that when blended with PHT, PHT plays nucleating roles for the crystallization of PHepT leading to higher crystallization rates of PHepT. Thus, it was of interests to investigate the nucleation effect of PHT crystals on the polymorphism of PHepT.

Fig. 6 shows DSC thermograms in PHT/PHepT blends with the higher PHepT content (PHT/PHepT = 0/100, 10/90, 30/70 and 50/

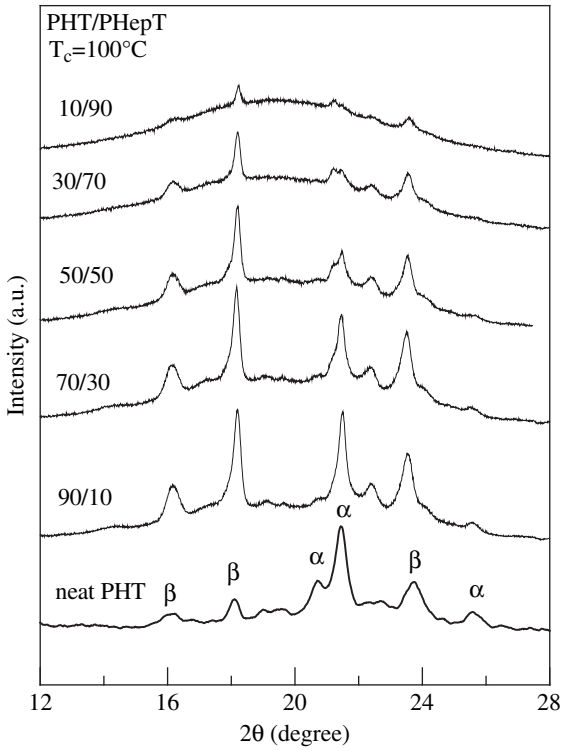

Fig. 5. WAXD diffractogrmas of PHT/PHepT blends melt-crystallized at 100 °C (measured at 100 °C).

50) melt-crystallized at (A) 60 °C and (B) 25 °C scanned with $R = 10$ °C/min. When heated at a $T_{max} = 180$ °C, which is high enough to erase all crystals or nuclei of PHT and PHepT, and quenched to these two temperatures, 60 and 25 °C, PHepT contains only the β- and α-crystal, respectively. In Fig. 6(A), the melting peaks corresponding to PHepT in all compositions show $P_{\beta 1}$ and $P_{\beta 2} + P_{\beta 3}$, indicating that the crystal form of PHepT in the PHT/PHepT blend crystallized at 60 °C remains β-crystal in the presence of PHT crystals. In Fig. 6(B), neat PHepT shows the melting peak of the α-crystal at 25 °C and upon blending with PHT, PHepT shows the melting peaks of the β-crystal. The blend samples upon heating at 180 °C and quenching to these two T_cs (60 and 25 °C) were also immediately scanned with a high scanning rate (100 °C/min) up to melting (data not shown fro brevity). The DSC curve shows only the melting peaks attributed to PHT, indicating that PHT is crystallized during the quenching process and thus plays a nucleating role for PHepT. This can be attributed to that the quenching rate of DSC is as high as 100 °C/min which may not be fast enough to suppress the crystallization of the fast-crystallized PHT. In addition, these two T_c's (60 and 25 °C) are much lower than the melting temperature of PHT leading to the great driving force for the crystallization of PHT during quenching. Consequently, results in this figure suggest that in the presence of PHT crystals, the β-crystal of PHepT in the miscible PHT/PHepT blend is preferentially crystallized at all T_c's. Thus, it is postulated that PHT crystals act as the nucleating agents which are preferentially favored by the β-crystal of PHepT.

3.3. Spherulite morphology in PHT/PHepT blend

Fig. 7 shows POM micrographs of the spherulite morphology in PHT/PHepT blend with various compositions melt-crystallized at $T_c = 100$ °C, which is higher than the melting temperature of PHepT (96 °C) and thus PHepT plays as amorphous diluents in the blends at 100 °C. Neat PHT shows the dual types of spherulites, in which one is the normal Maltese-cross spherulite attributed to the α-crystal (labeled as the α-spherulite) and the other is dendrite attributed to the β-crystal (labeled as the β-dendrite) [6]. In the blend with 10 wt% PHepT, the α-spherulite and β-dendrite similar to those in neat PHT are observed. However, with increasing PHepT content to 30 wt%, different dual types of spherulites are observed, in which one is irregular ringed and the other is ringless with Maltese-cross extinction. When blended with 50 or 70 wt% PHepT (PHT/PHepT = 50/50 and 30/70), PHT in the blends shows mixed ring-banded spherulites with regular ring-band patterns and normal Maltese-cross ones. In the PHT/PHepT = 10/90 blend, only ill-defined crystals are produced due to the low crystallizable PHT content in this composition. The insets in the bottom-left and bottom-right of the POM micrographs for the spherulite morphology of PHT/PHepT = 70/30 and 50/50 are the sketches of the irregular and regular ringed morphology, respectively, in which the ringed bands in the irregular spherulite of PHT/PHepT = 70/30 are more irregularly curved, while those in the regular ringed spherulites of PHT/PHepT = 50/50 are more regularly arc-like. When blended with PHepT, the dual types of spherulites in PHT are significantly altered and dependent on the PHepT content. In order to understand the original of the dual types of spherulites in PHT/PHepT blend and effects of the PHepT composition on the spherulite morphology of PHT, two blend compositions, PHT/

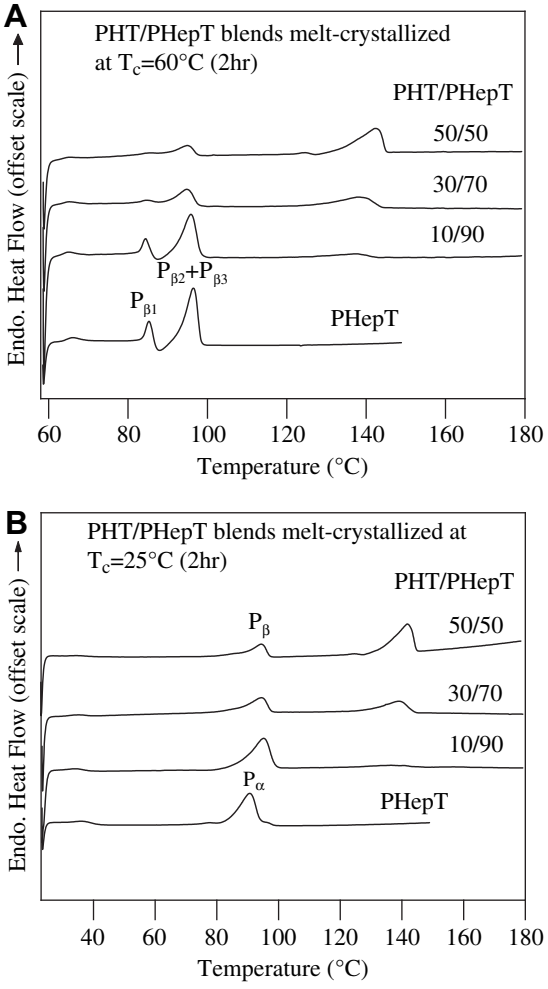

Fig. 6. DSC thermograms of PHT/PHepT blends (0/100, 10/90, 30/70 and 50/50) with higher fractions of PHepT melt-crystallized at (A) 60 °C and (B) 25 °C scanned at 10 °C/min.

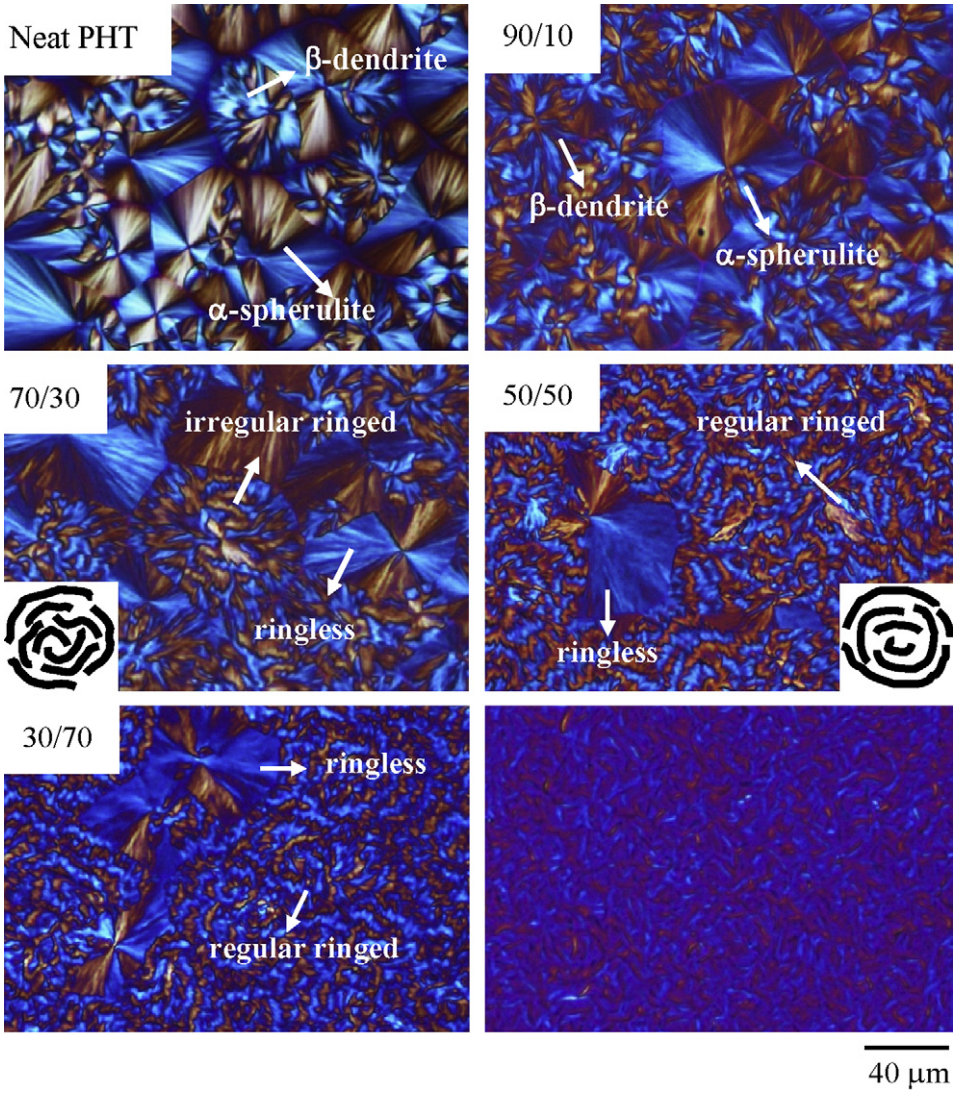

Fig. 7. Spherulite morphologies observed under POM in neat PHT and PHT/PHepT blends melt-crystallized at 100 °C.

PHepT = 70/30 and 30/70, were chosen as model blends and temperature-dependent WAXD and POM techniques were applied to clarify the correlations between the spherulite morphology and polymorphism in these two blends.

Fig. 8(A) shows temperature-resolved WAXD patterns in PHT/PHepT = 70/30 crystallized at 100 °C and heated to melt with heating rate = 1 °C/min. At 100 °C, the PHT/PHepT = 70/30 blend contains the mixed α- and β-crystal and upon heating to higher temperatures, the intensity of the diffraction peaks decreases gradually due to the melting of PHT crystals. When heated to 148 °C, only the diffraction peaks of the β-crystal ($2\theta = 17.9°$ and 23.6°) remain, indicating that at this temperature, the β-crystal is unmelted, whereas the α-crystal is melted. With further heating to 150 °C, the WAXD pattern shows a halo, indicating the complete melting of all crystals. Fig. 8(B) shows POM micrograph in PHT/PHepT = 70/30 melt-crystallized at 100 °C and the normal Maltese-cross and irregular ringed spherulites are observed. Fig. 8(C) is POM micrograph of sample-8(B) heated to 148 °C and then cooled back to 25 °C, which shows that the irregular ringed spherulites remain, but the normal Maltese-cross spherulites disappear. Besides, small crystals are produced in the location previously occupied by the normal Maltese-cross spherulites. It is supposed that upon heating from T_c to 148 °C to melt the α-crystal, the normal Maltese-cross spherulites melt and then during the cooling process to T_c, the small crystals are produced from the space originally occupied by the normal Maltese-cross spherulites. Consequently, the normal Maltese-cross spherulites are attributed to the α-crystal and the irregular ringed spherulites are attributed to the β-crystal.

Fig. 9(A) shows temperature-resolved WAXD patterns in PHT/PHepT = 30/70 crystallized at 100 °C and heated to melt with heating rate = 1 °C/min. At 100 °C, PHT/PHepT = 30/70 contains the mixed α- and β-crystal and when heated to higher temperatures, the intensity of the diffraction peaks decreases gradually due to the melting of PHT crystals. When heated to 145 °C, only the diffraction peaks of the β-crystal ($2\theta = 17.9°$ and 23.6°) remain, indicating that at this temperature, the β-crystal remains as solid, whereas the α-crystal is melted. Fig. 9(B) shows POM micrograph in PHT/PHepT = 30/70 melt-crystallized at 100 °C and the mixed normal Maltese-cross and regular ringed spherulites are observed. Fig. 9(C) is POM micrograph of sample-9(B) heated to 145 °C and then cooled to 25 °C, which shows that the regular ringed spherulites remain, but the normal Maltese-cross spherulites disappear. Besides, small crystals are produced in the location previously occupied by the normal Maltese-cross spherulites. When heated to

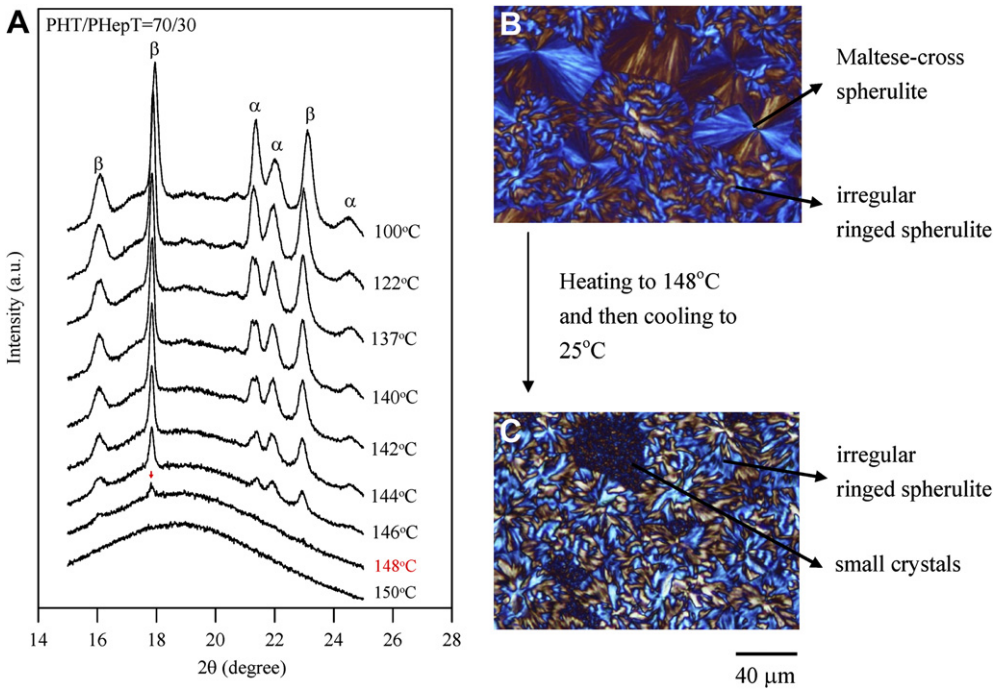

Fig. 8. (A) Temperature-dependent WAXD patterns of PHT/PHepT = 70/30 melt-crystallized at T_c = 100 °C and then heated to melt (1 °C/min), (B) POM micrographs in PHT/PHepT = 70/30 melt-crystallized at 100 °C, (C) sample-(B) heated to 148 °C and then cooled to 25 °C.

145 °C to melt the α-crystal, the normal Maltese-cross spherulites melt and then the small crystals are produced during the cooling process to T_c in the space originally occupied by the normal Maltese-cross spherulites. Consequently, the normal Maltese-cross spherulites are attributed to the α-crystal and the regular ringed spherulites are attributed to the β-crystal. To summarize the results in Figs. 8 and 9, the β-dendrite in neat PHT changes to irregular ringed and then to regular ringed spherulites with increasing PHepT content up to 70 wt% in the blends. However, the spherulite morphology packed of the α-crystal is not significantly influenced when blended with PHepT.

In miscible polymer blends comprising one semicrystalline polymer and one amorphous polymer, the effects of the amorphous component on the spherulite morphology of the other crystallizable component are interesting and have been studied in many cases [20–26]. Among aryl-polyesters, PET, PTT and PPT show ringed

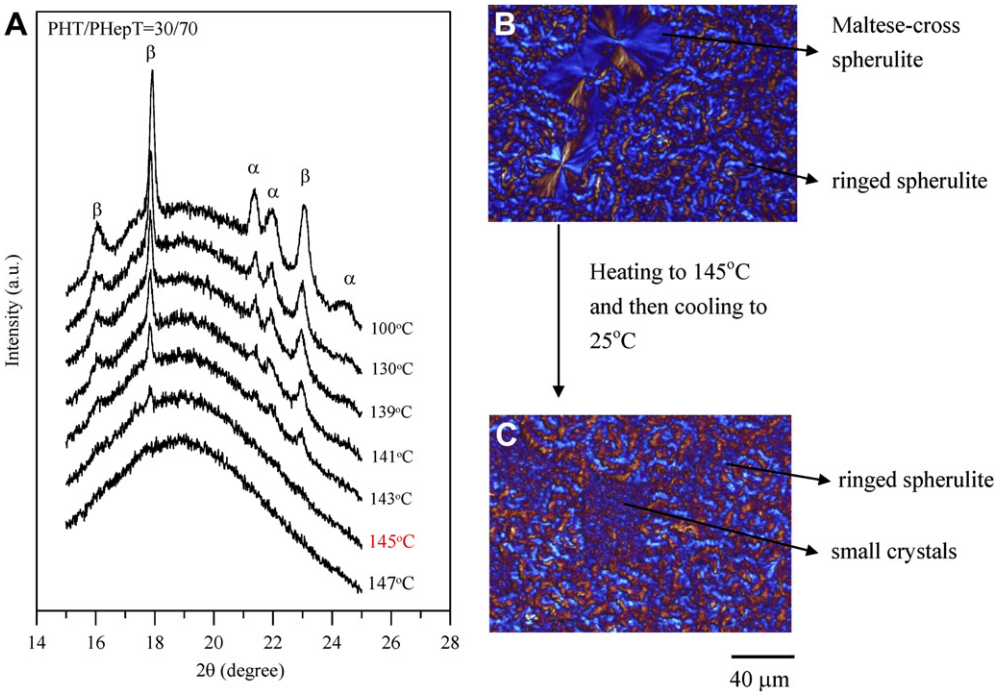

Fig. 9. (A) Temperature-dependent WAXD patterns of PHT/PHepT = 30/70 melt-crystallized at T_c = 100 °C and then heated to melt (1 °C/min), (B) POM micrographs in PHT/PHepT = 30/70 melt-crystallized at 100 °C, and (C) POM micrograph for sample-(B) heated to 145 °C and then cooled to 25 °C.

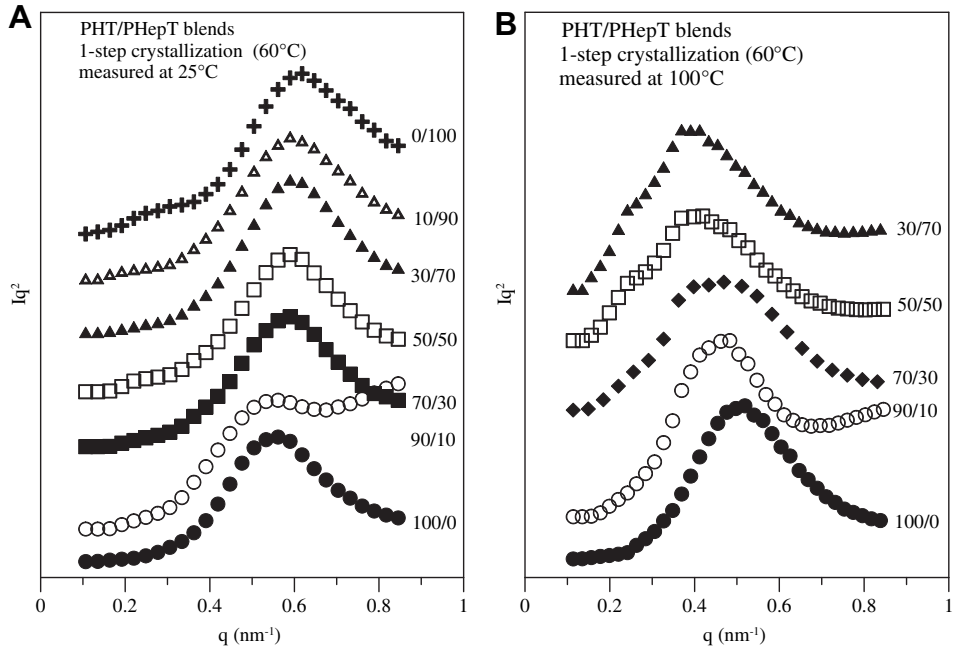

Fig. 10. SAXS profile of PHT/PHepT blends one-step crystallized at 60 °C (A) measured at 25 °C and (B) at 100 °C.

spherulites when melt-crystallize at certain temperature ranges. PTT exhibits ringed spherulites at $T_c = 150–210$ °C, and when blended with amorphous PEI component, the ring-band spacing of the ringed spherulites in PTT becomes smaller and the spherulite texture becomes coarse [20,21]. Neat PPT shows ringed spherulites at $T_c = 100–110$ °C; however, in its blends with PHepT contents higher than 30 wt%, the ringed PPT spherulites in blends crystallized at 100 °C become ringless [4].

Aliphatic polyesters also show interesting changes in spherulite morphology when blended with amorphous components [22–26]. Poly(ε-caprolactone) (PCL) exhibits ringed spherulites at T_c higher than 50 °C [22]. However in the miscible blend with amorphous polymers such as poly(vinyl methyl ether) (PVME), poly(phenyl methacrylate) (PPhMA), poly(benzyl methacrylate) (PBzMA) or poly(styrene-co-acrylonitrile) (SAN), PCL in these blends show ringed spherulites with more regular ring-band patterns [22]. In addition, the temperature ranges in the formation of the ringed spherulites of PCL in the blends shift to lower temperatures compared to that of neat PCL [22]. In contrast, upon blending with the bio-resourceful tannic acid (TA), only the normal Maltese-cross spherulites are observed at all T_c's in PCL/TA blend [19]. Poly(ethylene oxide) (PEO) shows the normal Maltese-cross spherulites at all T_c's, but when blended with strongly-interacted components, such as TA or poly(vinyl phenol) (PVPh), seaweed-like or dendritic morphology is observed in the blend of PEO/TA or PEO/PVPh = 70/30 [24,25]. However, if PEO is blended with a weakly-interacting amorphous component, the normal Maltese-cross spherulites of PEO in blends remain unchanged [26]. It is first time observed that the morphology changes from dendrite to ring-banded as in the PHT/PHepT blend.

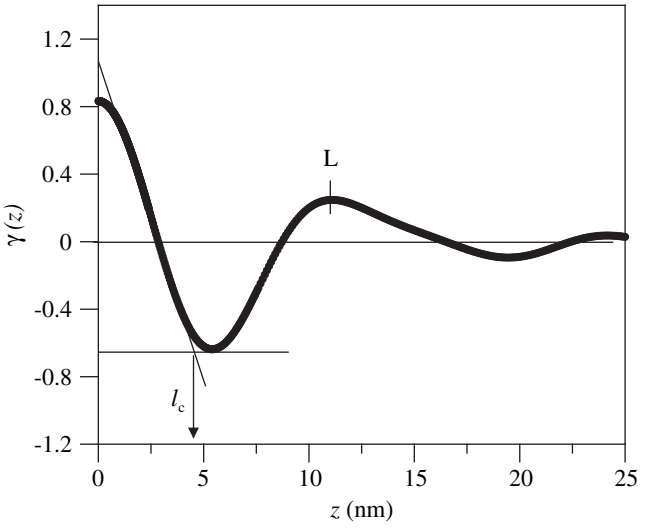

Fig. 11. One–dimensional correlation function of neat PHT homopolymer with L = long period, l_c = crystalline phase thickness, and l_a = amorphous phase thickness.

3.4. SAXS characterizations on PHT/PHepT blend

In a two-component semicrystalline/semicrystalline blend held at a T_c or upon cooling, the low-T_m component (PHepT) tends to solidify later than the high-T_m one. Thus, upon blend crystallization, the domain to which the low-T_m component can be confined depends on relative chain mobility of these two components, blend composition, and other crystallization conditions. For the PHT/PHepT blend, the chain mobility of PHepT in the blend does not change significantly due to the closely-spaced T_g values between these two components. The sole effect of PHepT composition on the segregation site of PHepT in the blend was analyzed on the one-step crystallized (60 °C) blend samples using SAXS. Fig. 10 shows the Lorentz-corrected SAXS profiles in PHT/PHepT blend (A) one-step crystallized at 60 °C (measured at 25 °C) and (B) sample-(A) heated to 100 °C (measured at 100 °C). At 60 °C, both PHT and PHepT are crystallizable and a three-phase system comprising the crystalline PHT, crystalline PHepT and amorphous phase is created. Fig. 10(A) shows the scattering peaks of neat PHT and PHepT are at $q = 0.55$ nm^{-1} and 0.6 nm^{-1}, respectively. There is only one scattering peak caused by the regular lamellar structure observed in each blend composition which shifts to the higher q value with increasing PHepT content. When heated to 100 °C to melt the

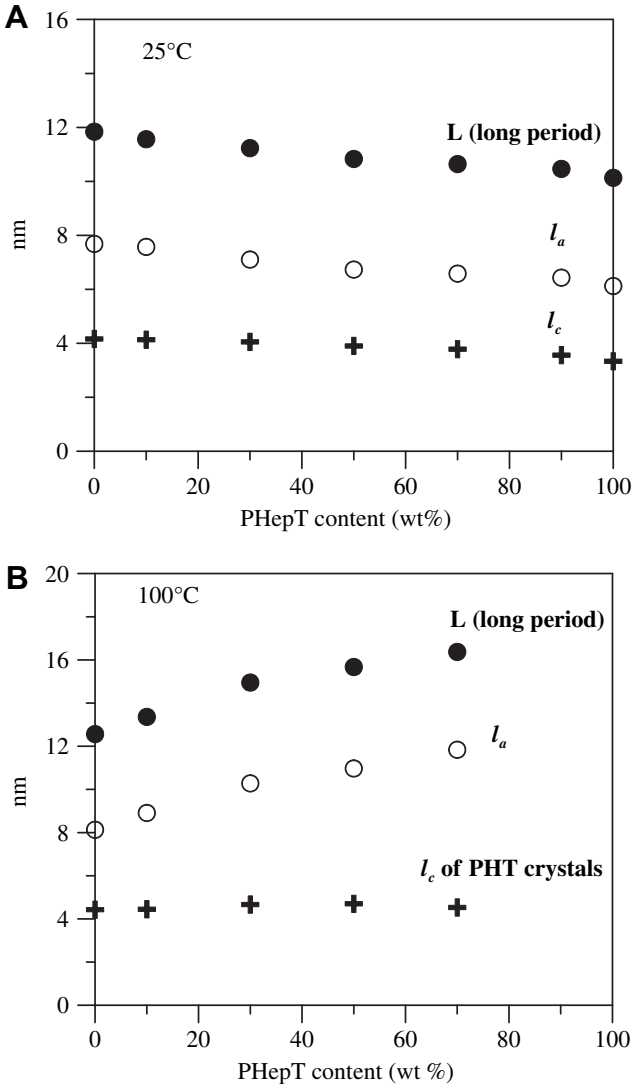

Fig. 12. Plots of average long period (L), average crystalline-phase thickness (l_c), average and amorphous-phase thickness (l_a) in PHT/PHepT blend one-step crystallized (A) at 60 °C and (B) sample-(A) heated to 100 °C.

PHepT crystals, the PHT/PHepT blend is in the semicrystalline/amorphous state. Fig. 10 (B) shows that the scattering peak of the blend shifts to the lower q value with increasing PHepT content. The scattering peak of neat PHT measured at 100 °C is at the lower q value compared to that measured at 25 °C, which may be attributed to the melting of the crystals with thinner lamellar thickness produced during secondary crystallization process. In semicrystalline polymer exhibiting the lamellar structure, the most common measurement from SAXS is the so-called long period, and the scattering signal comes from the difference in the electron density between the crystalline and amorphous phases. The electron density difference between the crystalline and amorphous phase ($\Delta\eta = \eta_c - \eta_a$) is correlated with the density difference between the crystalline and amorphous phase ($\Delta\rho = \rho_c - \rho_a$) of the component according to the equation: $(\rho_c - \rho_a) = (14/8)$(g/mol electron)$(\eta_c - \eta_a)$ [27]. The density of the crystalline and amorphous phase in PHT is 1.59 and 1.40 g/cm^3 [28], respectively, which gives $\Delta\eta_{PHT} = 0.108$ g/mole electron. Besides, the density of the crystalline and amorphous phase in PHepT is 1.56 and 1.38 g/cm^3 [28], respectively, which gives $\Delta\eta_{PHepT} = 0.103$ g/mole electron. Thus, the close-spaced value in $\Delta\eta$ of these two components may cause the indistinguishable detection of the individual scattering peak corresponding to PHT or PHepT. Thus, only one scattering peak is observed in each blend composition and the peak shifts to a higher q value with the addition of the lower-q component (PHepT). Upon heating to 100 °C, where only the PHT component remains solid, the down-shift in the q value of the scattering peaks with increasing PHepT content indicates that the distance between PHT lamellae increases. To investigate the PHT crystalline morphology at the lamellar level and the PHepT spatial distribution in the blend, the long period (L) and thickness of the crystalline phase (l_c) in PHT/PHepT blend crystallized at 60 °C and heated to 100 °C were determined using one–dimensional correlation function $\gamma(z)$, evaluated from the scattered intensity $I(q)$ by the flowing equation [12,29,30]:

$$\gamma(z) = \frac{2\pi^2}{Q}\int_0^\infty q^2 I(q)\cos(qz)dq \quad (1)$$

where z is the correlation distance along the direction from which the electron density distribution is measured and Q is the scattering invariant [12,28,29]:

$$Q = \frac{1}{2\pi^2}\int_0^\infty I(q)q^2 dq \quad (2)$$

Fig. 11 shows the typical correlation function of neat PHT, demonstrating how the long period (L), thickness of the crystalline phase (l_c), and thickness of the amorphous phase ($l_a = L - l_c$) are estimated from the correlation function curve. The first maximum is related to the long period (L) and the first minimum is corresponding to the thickness of crystalline phase (l_c) because the linear crystallinity of PHT is less than 50% [6,31].

Fig. 12 shows the plot of L, l_c and l_a in PHT/PHepT blend (A) one-step crystallized at 60 °C (measured at 25 °C) and (B) sample-(A) heated to 100 °C against PHepT content. At 25 °C, where both PHT and PHepT are crystallizable, L, l_c and l_a slightly decrease with increasing PHepT content. In contrast, at 100 °C, where PHepT is in the amorphous molten state, L and l_a increase with increasing PHepT content and l_c is nearly constant. In addition, L and l_a measured at 100 °C are higher than those measured at 25 °C, indicating that when the PHepT component in the blend melts, the average distance between PHT crystals increases. It is supposed that the PHepT component is incorporated in the PHT interlamellar region. In the blend with 50 wt% PHepT (PHT/PHepT = 50/50), the long period (L) is 11 nm at 25 °C while the long period at 100 °C is 16 nm, which is only 1.45 times larger than that at 25 °C. If PHepT is fully incorporated in PHT interlamellar region, the long period at 100 °C should be at least 2 times larger than that at 25 °C. Thus, the PHepT component may be partially excluded from the interlamellar region. By judging from the volume-filling spherulite morphology in PHT/PHepT = 50/50 melt-crystallized at 60 °C and then heated to 100 °C, the possibility of the interspherulitic region where PHepT resides is excluded. Consequently, in the PHT/PHepT blend, PHepT is located in both interlamellar and interfibrillar regions.

4. Conclusion

Crystalline/crystalline PHT/PHepT blend is miscible in the melt state or quenched amorphous glassy phase. Miscibility in the blend of two aryl-polyesters (PHT and PHepT) is proven by the homogeneous phase behavior as evidenced by single T_g and composition dependence of the cold-crystallization temperature ($T_{c.c.}$). Effects of miscibility on crystal growth kinetics, spherulite morphology, and polymorphism in the PHT/PHepT blend were analyzed. In the

miscible blend, the crystallization rates of PHT decrease and the thermodynamically stable β-crystal instead of the kinetically favorable α-crystal becomes dominant at $T_c = 100\ ^\circ C$. Besides, the dendrite of neat PHT packed of the β-crystal changes to the ringed spherulites when blended with PHepT content of higher than 50 wt%. Miscibility in PHT/PHepT blend also shows significant influence on the polymorphism of melt-crystallized PHepT, in which neat PHepT shows the α-crystal and β-crystal at T_c lower than 25 °C and higher than 35 °C, respectively. However, when blended with PHT, the β-crystal dominates at all T_c's. In addition, the crystallization rate of PHepT in the PHT/PHepT blend increases due to the nucleation effect of PHT crystals which are produced prior to the growth of PHepT crystals. For the PHT/PHepT blend either in a three-phase ($T < T_{m,PHepT} < T_{m,PHT}$) or two-phase system ($T_{m,PHepT} < T < T_{m,PHT}$), PHepT is spatially distributed in both PHT interlamellar and interfibrillar regions, which further clarifies the fine scales of homogeneity and the miscibility in this blend.

Acknowledgment

This work has been financially supported by a basic research grant (NSC-95 2221 E006 183) for three consecutive years from Taiwan's National Science Council (NSC), to which the authors express their gratitude. One of the co-authors, Ms. K.C. Yen, was trained for two weeks as an international exchange doctoral-program student at Department of Future Industry-Oriented Basic Science and Materials via funding generously provided by Toyota Technological Institute, Nagoya, Japan, where portion of the work in this study was performed.

References

[1] Kuo YH, Woo EM. Polym J 2003;35:236–44.
[2] Fakirov S, Evstatiev M, Petrovich S. Macromolecules 1993;26:5219–26.
[3] Yen KC, Woo EM, Chen YF. Polym J 2007;39:935–44.
[4] Yen KC, Woo EM, Chen YF. Polym Int 2009;58:1380–9.
[5] Woo EM, Kuo YH. J Polym Sci Part B Polym Phys 2003;41:2394–404.
[6] Ghosh AK, Woo EM, Sun YS, Lee LT, Wu MC. Macromolecules 2005;38:4780–90.
[7] Woo EM, Wu PL, Chiang CP, Liu HL. Macromol Rapid Commun 2004;25:942–8.
[8] Yen KC, Woo EM. Polymer 2009;50:662–9.
[9] Yen KC, Woo EM. J Polym Sci Part B: Polym Phys 2009;47:1839–51.
[10] Liu LZ, Chu B, Penning JP, Manley RStJ. Macromolecules 1997;30:4398–404.
[11] Penning JP, Manley RStJ. Macromolecules 1996;29:77–83.
[12] Penning JP, Manley RStJ. Macromolecules 1996;29:84–90.
[13] Chen HL, Wang SF. Polymer 2000;41:5157–64.
[14] Cheung YW, Richard SS, Chu B, Wu G. Macromolecules 1994;27:3589–95.
[15] Hall IH, Ibrahim BA. Polymer 1982;23:805–16.
[16] Palmer A, Poulin-Dandurand S, Revol JF, Brisse F. Eur Polym J 1984;20:783–9.
[17] Brisse F, Palmer A, Moss B, Dorset D, Roughead A, Miller DP. Eur Polym J 1984;20:791–7.
[18] Kawahara Y, Naruko S, Nakayama A, Wu MC, Woo EM, Tsuji M. J Mater Sci 2009;44:2137–42.
[19] Gilbert M, Hybart F. Polymer 1972;13:327.
[20] Lee JK, Choi MJ, Im JE, Hwang DJ, Lee KH. Polymer 2007;48:2980–7.
[21] Woo EM, Wu PL. Colloid Polym Sci 2006;284:357–65.
[22] Chen YF, Woo EM. Colloid Polym Sci 2008;286:917–26.
[23] Yen KC, Mandal TK, Woo EM. J Biomed Mat Res Part A 2008;86:701–12.
[24] Lin JH, Woo EM, Huang YP. J Polym Sci Part B Polym Phys 2006;44:3357–68.
[25] Yen KC, Woo EM. Polym Bull 2009;62:225–35.
[26] Wu L, Lisowski M, Talibuddin S, Runt J. Macromolecules 1999;32:1576–81.
[27] Strobl GR, Schenider M. J Polym Sci Polym Phys Ed 1980;18:1343–59.
[28] Van Krevelen DW. Properties of polymers. 3rd ed. Amsterdam: Elsevier; 1990.
[29] Strobl G. The physics of polymers: concepts for understanding their structures and behavior. 3rd ed. New York: Springer; 2007.
[30] Campbell D, White JR. Polymer characterization: physical techniques. Chapman & Hall; 1989.
[31] Sun YS. Polymer 2006;47:8032–43.